

## RF THERMAL PLASMA TREATMENT OF A FLUE DUST FROM THE SIEMENS-MARTIN PROCESS

I. MOHAI, J. SZÉPVÖLGYI and M. TÓTH<sup>1</sup>

(Research Laboratory of Materials and Environmental Chemistry, Chemical Research Center, Hungarian Academy of Sciences, Pusztaszeri út 59-67, Budapest, H-1025, HUNGARY

<sup>1</sup> Research Laboratory for Geochemistry, Research Center for Earth Sciences, Hungarian Academy of Sciences Budaörsi út 45, Budapest, H-1112, HUNGARY)

This paper was presented at the Second International Conference on Environmental Engineering, University of Veszprém, Veszprém, Hungary, May 29 – June 5, 1999

Recovery of iron, zinc and lead from a flue dust of 31.1% Fe, 17.4% Zn and 7.7% Pb content has been studied in an RF thermal plasma reactor under reducing conditions. Thermodynamic calculations based on the minimisation of Gibbs free enthalpy were made to estimate the product composition. Effects of the plate power of the RF generator and feed rate of powder on the chemical, surface, phase compositions and morphology of products have been investigated in details. It has been proved that the RF thermal plasma treatment makes it possible to recover a considerable part of zinc and lead from the particular dust on the one hand, and a product of increased iron content can be produced on the other hand.

**Keywords:** RT plasma; metallurgical waste; reduction; XRD; XPS; SEM

### Introduction

Steel-making dusts tend to be rich in zinc and lead because of the use of galvanised and other zinc-containing scrap in the charge. Processes developed for the processing of particular dusts, however, do not provide economic recycling. These dusts are mostly regarded as hazardous wastes due to the leaching of their toxic constituents on dumping.

Application of the RF thermal plasma technology in the waste management is based on the ability to deliver high-grade heat independently of the oxygen potential. Compact units of high output can be constructed, and they are able to handle cheap feed stock with a minimum environmental impact [1].

The commercial plasma processes developed for the recycling of ferrous wastes are mainly based on arc plasmas and they usually require granulated raw materials. Among others, PLASMADUST system by SKF (combination of a plasma gas heater with a coke-filled shaft furnace) and TRD (Tetronics Research and Development) process (smelting in a transferred-arc furnace) [2] belong to these technologies. In PLASMAREC process [3] the plant can easily be mobilized and transported to the required site to eliminate e.g. local contamination.

The RF thermal plasmas make it possible to ensure any required (oxidative, reducing or neutral) atmosphere for high temperature reactions, independently of the temperature. It is a very attractive feature in terms of waste processing. In this paper the application of a RF thermal plasma system for the treatment of a ferrous dust in reducing conditions is investigated.

### Experimental

A dust separated from the flue gas of a Siemens-Martin furnace (SM-dust) was treated in a laboratory size RF thermal plasma reactor with a quartz-glass confinement tube of 2.8 cm inner diameter. The RF generator operated at 27 MHz with a continuous adjustment of the plate power in the range of 1 to 7 kW. The reactor was connected to an air cooled, two-stage powder collector. Argon was used as the central plasma gas ( $7 \text{ dm}^3 \text{ min}^{-1}$ ) and as the sheath gas ( $19 \text{ dm}^3 \text{ min}^{-1}$ ), as well. The powder was injected into the plasma reactor by an argon carrier gas passed through a fluidised and vibrated powder-bed. Hydrogen used as reducing agent was injected into the plasma tail flame region with a feed rate of  $1 \text{ dm}^3 \text{ min}^{-1}$ . A more detailed description of the plasma reactor was published previously [4].

Table 1 Conditions of thermal plasma treatment

Run	Spec. energy ( $\text{kWh g}^{-1}$ )	Plate power (kW)	Powder feeding rate ( $\text{g h}^{-1}$ )	Reactor type*
1	0.16	2.4	15.0	A
2	0.3	2.8	10.2	A
3	0.4	2.5	6.4	B
4	0.69	3.0	4.3	A
5	0.75	2.2	2.9	D
6	0.95	2.4	2.6	B
7	0.95	2.5	2.6	B
8	1.0	3.0	3.0	A
9	1.1	2.7	2.6	A
10	1.6	3.0	1.9	A
11	1.6	2.5	1.6	B
12	0.13	2.1	15.8	E

\* A: powder feeding into the plasma gas, B: powder feeding into the tail flame region through two radial inlets, D: powder feeding into the tail flame region through one tangential inlet, E: hot wall reactor

The experimental conditions are listed in Table 1. In the second column of Table 1, the specific energy calculated as the ratio of plate power to the powder feed rate is presented. Hence, this parameter considers two process variables simultaneously.

The raw material and the products as well were characterised in terms of particle size, bulk and surface chemical compositions, phase conditions and morphology. In each run products were collected both from the reactor (R) and from the dust collector (C).

Particle size distribution was measured by a Particle Size Analyser (Malvern 2600C). Bulk chemical compositions were measured on dissolved samples by ICP-AES technique (Labtest PSX7521). Surface chemical compositions were characterised by X-ray photoelectron spectroscopy (XPS, Kratos XSAM800). Phase conditions were determined by X-ray diffraction analysis (XRD, Philips PW 1710). Morphology was investigated using scanning electron microscope (JEOL JSM50A).

## Results and Discussion

### Characterisation of the Starting Material

According to the particle size analysis the original SM-dust has a broad particle size distribution between 1-200  $\mu\text{m}$  with a mean particle size of 4.6  $\mu\text{m}$ . As particles above 10  $\mu\text{m}$  in diameter can not evaporate completely in the plasma due to the short residence time, prior to the reduction the SM dust was milled in a Fritsch mill. The resulted powder had a mean particle size of 1.9  $\mu\text{m}$  with a distribution from 0.5 to 18  $\mu\text{m}$ .

Chemical composition of the SM-dust was determined by ICP-AES after dissolution in diluted  $\text{HNO}_3$  in a microwave digestion system. Main components of particular dust are Fe: 31.1%, Zn: 17.4%, Pb: 7.7%. The minor (0.1-1%) elements include Si, Al, Ca, Mg, Cr, Ni, Mn, Cu, Cd, and Sn. The SM dust contains non-metallic components, such as: S: 5.5%, P: 0.4%, C: 0.6%, Cl: 1%, F<1%. According to

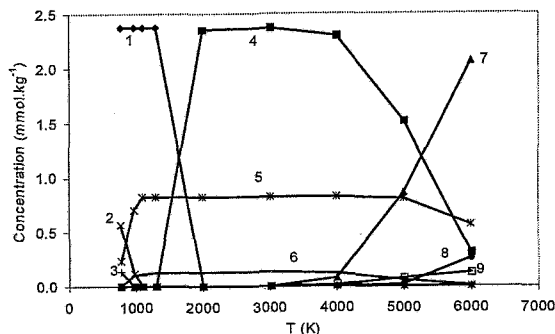


Fig.1 Equilibrium compositions as the function of the temperature at atmospheric pressure (feeding rate of SM dust:  $1 \text{ g h}^{-1}$ ). Assignment: 1: Fe(s,l), 2: ZnS(s,l), 3: Pb(s,l), 4: Fe, 5: Zn, 6: Pb, 7:  $\text{Fe}^+$ , 8:  $\text{Zn}^+$ , 9:  $\text{Pb}^+$

the XPS investigations the sample is covered by a surface oxide layer.

The main crystalline phases of the SM-dust were franklinite ( $\text{ZnO}\cdot\text{Fe}_2\text{O}_3$ ) and magnetite ( $\text{FeO}\cdot\text{Fe}_2\text{O}_3$ ). Traces of other Zn-containing phases such as zincite (ZnO) and sphalerite (ZnS) were also detected. The lead was present in the original powder as plattnerite ( $\text{PbO}_2$ ). Minor amounts of other iron containing phases such as wüstite (FeO) and pyrrhotite (FeS) were also detected.

### Thermodynamic Calculations

The thermodynamic calculations are of outstanding importance in the particular case, because in thermal plasma reactors the first condensed phase that appears on cooling will be the dominant phase of the products. The high cooling rate in thermal plasmas does not make possible reactions involving liquid or solid phases. The equilibrium compositions as a function of temperature (in the range of 773-6000 K) during reduction of the SM dust with hydrogen were calculated by the use of a computer program based on the minimisation of the Gibbs free enthalpy [5]. Assuming a feed rate of  $1 \text{ g h}^{-1}$  SM dust,  $60 \text{ dm}^3 \text{ h}^{-1}$   $\text{H}_2$  and  $1740 \text{ dm}^3 \text{ h}^{-1}$  argon, the equilibrium composition of the elements, ions and compounds can be seen in Fig.1. Although in the calculations all analysed components were considered, only the Fe, Zn and Pb containing compounds are represented in Fig.1. On cooling of the gaseous species formed in the plasma flame region the first condensed phase that appears below 2000K is Fe(s,l). Minor amount of silicates, Mn and Ca sulphides and  $\text{Cr}_2\text{O}_3$  condensate, as well. When Zn vapours start to condensate below 1100K ZnS and some ZnO may be formed because of the relatively high concentration of  $\text{H}_2\text{O}$  and  $\text{H}_2\text{S}$  vapour in this temperature range. When  $\text{H}_2\text{S}$  concentration decreases ( $T < 800\text{K}$ ) condensation of metallic zinc is also probable. Pb content of the starting material condensates in metallic form below 973 K. Increasing the feed rate of powder from  $1 \text{ g h}^{-1}$  to  $15 \text{ g h}^{-1}$  results in 100-200K higher condensation temperatures of the metal vapours. In this case in addition to metallic Fe, FeS appears as well. To

Table 2 Results of the thermal plasma treatment of SM dust

Run	$E_{sp}$ (kWh g <sup>-1</sup> )	Sample	Fe (wt %)	Zn (wt %)	Pb (wt %)	$\Sigma(\text{Fe}+\text{Zn}+\text{Pb})$ (wt %)	Fe/Zn (%/%)
0	0	SM	31.1	17.4	7.7	56.2	1.8
1	0.16	R	34.5	20.9	9.3	64.7	1.7
		C	36.5	20.5	7.9	64.9	1.8
2	0.3	R	45.1	17.3	6.5	69.0	2.6
		C	36.9	23.9	7.3	68.1	1.5
3	0.4	R	45.1	16.0	7.3	68.4	2.8
		C	34.0	25.6	8.7	68.3	1.3
4	0.69	R	47.3	13.2	7.2	67.7	3.6
		C	32.0	30.3	8.9	71.2	1.1
5	0.75	R	47.2	18.3	8.1	73.6	2.6
		C	30.0	28.8	9.2	68.0	1.0
6	0.95	R	46.6	15.9	6.4	68.9	2.9
		C	36.8	24.1	8.0	68.9	1.5
7	0.95	R	49.3	12.5	6.9	68.3	3.9
		C	25.5	36.7	9.9	72.1	0.7
8	1.0	R	53.1	14.5	6.1	73.7	3.7
		C	32.2	30.2	7.1	69.5	1.1
9	1.1	R	46.0	15.4	8.6	70.0	3.0
		C	33.4	25.7	6.1	65.2	1.3
10	1.6	R	51.2	13.4	5.3	69.8	3.8
		C	27.2	33.8	9.5	70.5	0.8
11	1.6	R	55.1	12.0	5.9	73.0	4.6
		C	35.5	25.6	7.7	68.8	1.4
12	0.13	R1	68.1	4.3	3.3	75.7	15.8
		R2	18.8	43.2	12.5	74.2	0.4
		C	15.0	51.5	12.4	78.9	0.3

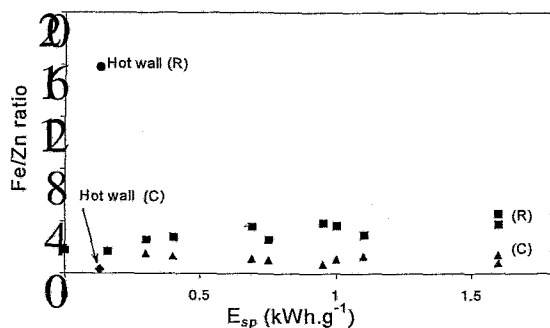


Fig.2 The Fe/Zn ratio as the function of specific energy  
C: samples from the collector, R: samples from the torch

conclude it all: in the given system metallic Fe, Pb and some Zn can be formed as a result of complete reduction. Appearance of ZnS and ZnO, and at higher feed rates of powder that of FeS can be expected, as well.

### Reduction of Model Compounds

As the chemical composition of the SM dust was rather complex studies on the reduction started with simple model compounds, such as Fe<sub>2</sub>O<sub>3</sub>, ZnO and a Fe<sub>2</sub>O<sub>3</sub>+ZnO mixture. The latter had an Fe/Zn ratio similar to the SM dust. According to the changes of the standard molar free enthalpy of the model compounds in the function of temperature, reduction of ZnO with hydrogen needs higher temperature (>1500K) than that of Fe<sub>2</sub>O<sub>3</sub> (>900K). However, reduction rate for ZnO was more than 95%, while for Fe<sub>2</sub>O<sub>3</sub> it was only 88% on thermal plasma treatment. The contradiction between

the thermodynamic calculations and experimental data can be reasoned by the different mean particle sizes of ZnO and Fe<sub>2</sub>O<sub>3</sub> (3.7 μm and 11.4 μm, respectively). Reduction of the Fe<sub>2</sub>O<sub>3</sub>+ZnO mixture resulted in a metallization of 86-90%. It is worth mentioning that a complete metallization can not be reached because the ultradisperse particles condensed from the vapour phase tend to oxidize during handling in the ambient air (e.g. fine iron particles collected from the reactor started to ignite spontaneously when contacted with air).

### Results of the Plasma Treatment

In the plasma reduction tests four different reactor constructions were used (Table 1). In reactor A powder was fed into the argon plasma gas. This operation is similar to that of analytical ICP torches, and utilizes the heat of the plasma with a good efficiency. However, in our case the plasma flame became unstable during this operation, due to the difficulties in the steady feeding of the particular powders. Reactor B had two radial inlets for powder feeding into the plasma tail flame region. However, the bent inlets tended to clog. For this reason reactor D had only a single inlet. It was tangential in order to extend the residence time in the hot zone of the reactor. To reduce the heat loss, and hence to ensure the so-called "hot-wall" conditions, reactor D was covered in a test by a refractory lining (reactor E). Unfortunately, the insufficient cooling in reactor E impedes longer reaction periods because the quartz reactor wall can be damaged.

The bulk chemical composition of plasma treated samples indicates an increasing reduction rate with specific energy (Table 2. Runs 1-11). Samples collected from the reactor wall (R) have higher Fe and lower Zn content as compared to samples C collected from the dust collector. It is explained by the gradual decrease in the temperature of the reactor wall and the powder collecting system with the distance from the plasma flame. This phenomenon makes possible the selective condensation of metals with different boiling points. In the case of  $E_{spec} = 1.6 \text{ kWh g}^{-1}$  the Fe/Zn ratio of 1.8 of the SM powder (Fig.2) increased to 4.6 for the sample R from Run 11. However, it decreased to Fe/Zn = 0.7 in sample C from Run 7. The segregation improved further when the heat loss of reactor was reduced by the refractory lining (Run 12). In this experiment, when  $E_{spec}$  was  $0.13 \text{ kWh g}^{-1}$ , Fe/Zn ratio was 15.8 in sample R1 and 0.3 in sample C. We would like to emphasize that in Run 12 a specific energy amounting less than 10% of  $E_{spec}$  of Run 11 was applied. In Run 12 two samples were collected from the reactor: R1 from top section, near the plasma flame, and R2 from the bottom of the reactor. Such sampling made it possible to investigate the changes in Fe and Zn concentrations with the distance from the injection point of the dust (Fig.3). Sample R1 from Run 12 had high Fe (68.1%) and low Zn (4.3%) contents. By increasing the distance, a region with no powder deposition could be observed

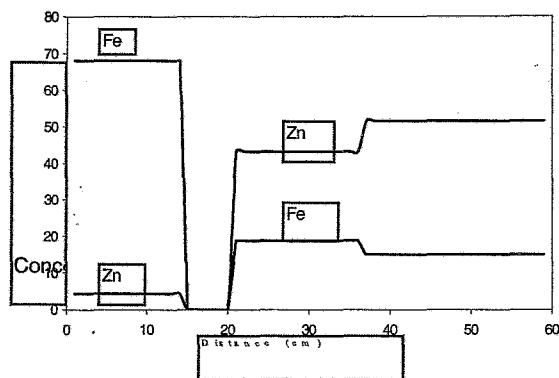


Fig. 3 Changes in the concentration of Fe and Zn against the distance from the SM dust inlet tube (Run 12)

in the hot wall (E) reactor. The existence of such powder free region refers to different condensation mechanisms in the upper and lower parts of the reactor, respectively. GIRSCHICK [6] considers that particles deposited on the wall near the plasma flame are formed by an ion-induced nucleation mechanism. However, at lower sections the particles are formed by homogenous nucleation from the vapor phase convecting downwards axially. We suppose that in our system, where the condensation temperatures of components are rather different, even heterogeneous nucleation can not be excluded.

Samples R2 and C from Run 12 have higher Zn and lower Fe content than sample R1 (Fig. 3). However, contrary to our expectations, the Fe content can not be lowered to zero in sample C. Most probably, the mass transport by convection depressed the segregation of Fe and Zn in this case.

Samples R2 and C from Run 12 have higher Zn and lower Fe content than sample R1 (Fig. 3). However, contrary to our expectations, the Fe content can not be lowered to zero in sample C. Most probably, the mass transport by convection depressed the segregation of Fe and Zn in this case.

Significant Pb segregation between samples R and C could only be observed in Run 12 (hot-wall reactor) because of the high boiling point of Pb (1620°C).

The XPS investigations of original and thermal plasma treated SM dusts indicated that both powders were covered by an uppermost surface oxide layer. Hydrocarbon-type surface carbon contamination was also detected in all samples. Surface compositions were calculated by taking into account the carbon contamination [7]. The bulk and surface compositions were referred to 1 mole Fe<sub>2</sub>O<sub>3</sub> in order to facilitate their comparison (Table 3).

A considerable surface segregation of zinc and lead was observed both in the original SM-dust and in the reduced powders produced therefrom. However, the thermal plasma treatment increased segregation. An especially high surface enrichment of ZnO was detected in Sample 4C. Although calculations on surface composition referred to oxides, occurrence of ZnS is very probable especially in sample 4R (molar ratios of ZnO and SO<sub>3</sub> are very close to each other). However, ZnO and ZnS can not be distinguished in the XP spectra, because they practically have the same chemical shift.

Both the bulk chemical composition of the treated samples and the XRD results (see below) refer to the

Table 3 Bulk and surface molar ratios related to Fe<sub>2</sub>O<sub>3</sub>

Sample	Fe <sub>2</sub> O <sub>3</sub>	ZnO	PbO <sub>2</sub>	SiO <sub>2</sub>	K <sub>2</sub> O	Cl	SO <sub>3</sub>	r*
SM bulk	1.0	1.0	0.1					
SM surf.	1.0	9.6	1.2	2.3	0.0	2.7	2.1	1.3
4R bulk	1.0	0.5	0.1					
4R surf.	1.0	6.2	2.2	2.3	2.0	2.0	6.5	0.9
4C bulk	1.0	1.6	0.1					
4C surf.	1.0	37.9	4.1	2.9	0.9	7.1	11.3	0.7

\* Ratio (O<sub>M</sub>/O<sub>C</sub>) of the measured and calculated amount of oxygen.

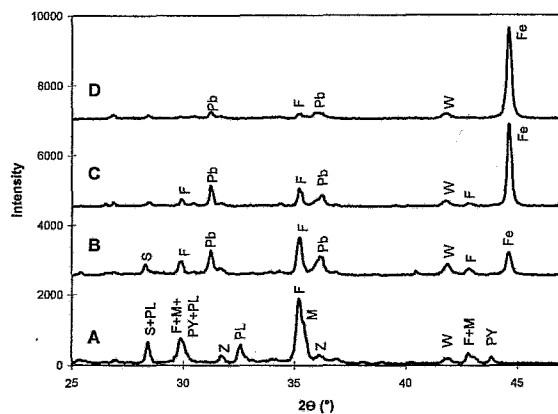


Fig. 4 X-ray diffractograms of SM-dust (A) and of plasma treated samples R for specific energies of 0.16 kWh g<sup>-1</sup> (B), 0.69 kWh g<sup>-1</sup> (C) and 1.00 kWh g<sup>-1</sup> (D). Assignment of peaks: F-franklinite, M-magnetite, W-wüstite, PY-pyrrhotite, PL-plattnerite, S-sphalerite, Z-zincite, Fe-iron, Pb-lead

reduction of ZnO-Fe<sub>2</sub>O<sub>3</sub>. Therefore, the surface enrichment of ZnO in the plasma-treated sample 4C can be traced back to the condensation and subsequent oxidation of Zn vapour on the surface of iron-rich nuclei. Changes in the ratio of the measured and calculated amount of oxygen also refer to reduction.

X-ray diffraction patterns of plasma-treated samples collected from the reactor indicated a significant decrease in the intensity of the franklinite, magnetite, zincite and plattnerite peaks, even at the lowest specific energy used in these tests. At higher energies further decrease of the franklinite with a simultaneous increase of the metallic Fe was observed (Fig. 4). However, the intensity of the metallic Pb peak in R samples decreased in some extent with the specific energy due to a partial segregation of lead. Zinc content of franklinite was probably transformed into a quasi-amorphous material in terms of XRD analysis: in spite of the considerable amount of Zn in the bulk and on the surface, no XRD peaks of metallic Zn, zincite or sphalerite could be detected. The zinc containing phase might form a thin surface layer, which is transparent to the X-rays.

XRD intensity of the wüstite peak actually did not change during the thermal plasma treatment. The wüstite phase is probably located in the core of the grains.

Samples R and C have quite different morphology (Fig. 5). Sample R, which was deposited on the reactor wall, mainly consists of large, agglomerated particles.

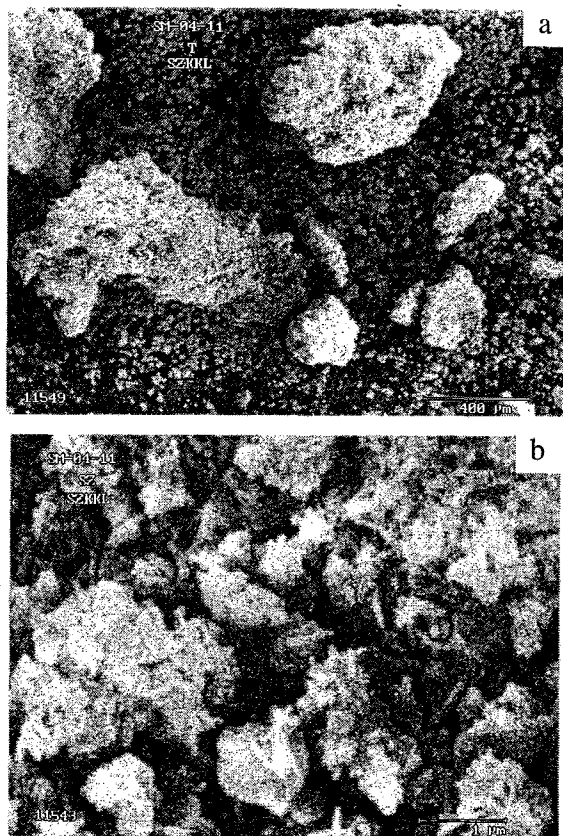


Fig.5 SEM micrographs of plasma reduced samples 4R (a) and 4C (b)

On the contrary, sample C has rather uniform, fine particles, which form loose agglomerates. The agglomeration most probably occurred after deposition, not during the flight [6]. Therefore the high temperature of the reactor wall in the case of samples R accelerated the agglomeration.

### Conclusions

The RF thermal plasma treatment of an oxidic SM-dust in a hydrogen flow makes it possible to reduce its iron, zinc and lead oxide content. The extent of reduction greatly depends on the plate power, and hence the specific energy related to unit feed rate of powder.

Products collected from the different parts of the experimental set-up have different compositions. The

further is collected the powder from the plasma flame, the higher is its zinc content. In the high temperature zones powders of high iron content were separated.

A considerable surface segregation of zinc and lead was detected even in the original SM-dust. Thermal plasma treatment resulted in products of even less uniform composition: zinc and lead were concentrated near to the surface of grains. The products are susceptible to surface oxidation.

The sulphur content of SM dust has a disadvantageous effect on the reduction with hydrogen due to zinc sulphide formation even at low  $H_2S$  tension.

### Acknowledgement

The authors are grateful for the financial support from the OTKA Fund (No. F016178). The authors would also like to thank to Mr. FERENC TILL for the particle size analysis, to Mr. MIKLÓS MOHAI for the XPS measurements and to Ms ZSUZSA FARKAS for preparing SEM micrographs.

### REFERENCES

1. HARE A.L.: Non-ferrous Metals and Miscellaneous Applications of Plasma Technology. In Plasma Technology in Metallurgical Processing (Ed. J. FEINMAN) ISS, Warrendale, PA, 1987, pp. 175-184
2. ERIKSSON S., JOHANSSON B. and SANTEN S.: Application of Plasma Technology to Steelplant Waste Treatment. In Plasma Technology in Metallurgical Processing (Ed. J. FEINMAN) ISS, Warrendale, PA, 1987, pp.125-130
3. HOFFELNER W., BURKHARD R., HAEFELI V. and SUN H.: Application of Thermal Plasma for Recovery of Metals and Destruction of Waste. Proc. 13-th International Symposium on Plasma Chemistry, Beijing, China, pp. 1915-1919, 1997
4. SZÉPVÖLGYI J. and MOHAI-TÓTH I.: *J.Mater.Chem.*, 1995, 5 (8), 1227-1232
5. BALMAEVA L.M., LAINER J.A., BABIEVSKAYA I.Z. and KRENEV V.A.: *Zh. Neorg. Khim.* 1994, 39 1292-1297.
6. GIRSHICK S.L., CHIU C.-P., MUNO R., WU C. Y., YANG L., SINGH S.K. and MCMURRY P.H.: *J. Aerosol Sci.*, 1993, 24 (3), 367-382
7. MOHAI M and BERTÓTI I.: Correction for Surface Contaminations in XPS: A Practical Approach. Proc. ECASIA 95 (Eds. H.J. MATHIEU, B. REIHL, D. BRIGGS), John Willey & Sons, Chichester-New York-Brisbane-Toronto-Singapore, 1995, pp. 675-678